Hydrodynamic and Thermodynamic Behavior of Short-Chain Polystyrene in Toluene and Cyclohexane at 34.5 °C†

Klaus Huber, Siegfried Bantle,‡ Pierre Lutz,§ and Walther Burchard*

Institute of Macromolecular Chemistry, University of Freiburg, D-7800 Freiburg, FRG.
Received November 28, 1984

ABSTRACT: Diffusion coefficients, radii of gyration, and second virial coefficients of short polystyrene chains have been measured by dynamic light scattering, small-angle neutron scattering, and static light scattering. Deviations from the established exponential laws at high molecular weights are observed in all cases. The hydrodynamic behavior can equally well be described by Kirkwood's diffusion equation, if the free draining term is properly taken into account, and by the Yamakawa–Fujii theory of cylindrical wormlike chains. The enhanced increase of A_2 for short chains is caused by the inherent chain stiffness. Satisfactory agreement of the Stockmayer–Yamakawa theory with experiment is obtained if a 45% higher Kuhn length is assumed in toluene at 20 °C than in cyclohexane at 34.5 °C.

Introduction

Polystyrene (PS) is probably the most extensively investigated linear-chain molecule in polymer science, and no really new results may be expected, in particular since recent measurements in different laboratories have given quite good experimental agreement. A new situation occurred, however, with the facilities of small-angle neutron scattering (SANS) and recent development in dynamic light scattering (DLS), which allow very accurate measurements of the geometric and hydrodynamic properties, and these measurements can be extended to the rather low molecular weight of $M_w \sim 1000$.

This region of low molecular weight is of particular interest, since deviations from Gaussian statistics may become apparent. These deviations are caused by the rotational hindrance of the monomer units and the resulting chain stiffness. The hydrodynamic behavior may in addition to this be influenced by the friction of the individual units, which for long chains play no role in comparison to the hydrodynamic interaction among the various units. Chain stiffness has influence also on the second virial coefficient, which to date is not yet fully understood.

In a previous paper[1] we carried out measurements of the translational diffusion coefficient D for poly(methyl methacrylate) (PMMA) in a good and a Θ solvent. While in the high molecular weight region the already well-known scaling behavior was obtained,[25] but now with higher accuracy, we found in the low molecular weight region, i.e., $M_w < 6 \times 10^4$, deviations from the simple exponential law. This gave rise for a similar investigation with PS low molecular weight solutions.

The expansion factor of random coils, due to excluded volume effects, is defined by Flory[26] as the ratio of the radii of gyration in a good and a Θ solvent, respectively.[25]

$$\alpha_S = \langle S^2 \rangle_z^{1/2} / \langle S^2 \rangle_{z\Theta}^{1/2} \quad (1)$$

SANS enables us now to investigate experimentally this expansion in the low molecular weight region, and these results can be used for interpreting the second virial coefficient quantitatively.

With the design of a special photogoniometer, we have the facility to record dynamic and static light scattering (SLS) measurements simultaneously; i.e., DLS and SLS are performed with the same solution at the same time. These simultaneous measurements provide us in principle with six relevant quantities, i.e., M_w, $\langle S^2 \rangle_z$, A_2, D_z, $C\langle S^2 \rangle_z$, and k_D, where C is a dimensionless quantity that is characteristic for the chain architecture and polydispersity,[27] and k_D is the coefficient in the concentration dependence of D:

$$D_{app}(c) = D_z(1 + k_D c) \quad (2)$$

By means of LS the mean square radius of gyration $\langle S^2 \rangle_z$ and the coefficient C can be determined for large molecular weight samples only, but M_w, D_z, A_2, and k_D can be measured over the whole molecular weight region. In this paper a quantitative description of these data at low molecular weight is attempted on the basis of current theories.

Experimental Section

Polymers. Samples A1-1 and A1-2 were prepared by anionic polymerization in benzene in our laboratory. Samples PS-3 and PS-1 were synthesized by one of us in Strasbourg, and samples H-1 and H-2 were kindly supplied by Professor H. Höcker, University of Bayreuth.

Samples PCC-4 and PCC-50 are products of Pressure Chemical Co., Pittsburgh, PA, sample WA-411 was supplied by Waters Associates, Framingham, GB, and TSK-11 is a product of Toyo Soda Manufacturing Co. Ltd., Tokyo, Japan.

The polydispersity index M_w/M_n in no case was larger than 1.1.

Static and Dynamic Light Scattering. The light scattering measurements were carried out with an apparatus that allows the simultaneous recording of SLS and DLS, as was described elsewhere.[3] A Model 165 krypton laser (Spectra Physics) was used as light source (λ = 647.1 nm) for all but two samples. For PS-3 and PS-1 measurements were performed with a Model 165 argon ion laser (Spectra Physics) (λ = 514.5 nm).

To yield DLS data, the scattered light was evaluated by an autocorrelator (Malvern K7023) with 96 channels, of which 72 channels were used for the construction of the time correlation function. The last 20 channels, delayed by 164 sample times, are taken for the determination of the base line. In all measurements the base line was compared with the "far point" calculated by the correlator.

The dn/dc measurements were performed with a KMX-16 Chromatix differential refractometer, operating at 633 nm, or with a Brice Phoenix differential refractometer at 436, 546, and 633 nm. The data are listed in Table I. For molecular weights higher than 15 000 a constant value of 0.106 cm^3/g in toluene and 0.167 cm^3/g in cyclohexane was found for λ = 633 nm.

Toluene and cyclohexane used for light scattering experiments and dn/dc measurements were distilled over sodium wire. The polymer solutions were clarified by centrifugation of the scattering cells in a swinging-bucket rotor with the floating technique.[37]

SANS Measurements. Measurements were performed at the Institut Max von Laue-Paul Langevin (ILL), Grenoble, France. All experiments were carried out with the D-17 instrument, where a 64 × 64 cell matrix assembly[35] is used for detecting the scattering

† This paper is affectionately dedicated to Professor R. Koningsveld, DSM, Geleen, on the occasion of his 60th birthday.

‡ Institut Laue-Langevin, Grenoble, France; present address: Sandoz AG, Basel, Switzerland.

§ Centre de Recherches sur les Macromolecules, Strasbourg, France.

0024-9297/85/2218-1461$01.50/0

Table I
dn/dc (g cm^{-3}) Measurements for Linear PS in Toluene at 20 °C and Cyclohexane at 34.5 °C

		toluene			cyclohexane		
sample	M_w	633 nm	546 nm	436 nm	633 nm	546 nm	436 nm
TSK-11	10700	0.105			0.168		
PCC-4	4000	0.102			0.166		
PS-3	3100	0.0956	0.0961	0.0980	0.160	0.165	0.176
PS-1	1200	0.0891	0.0901	0.0930	0.156	0.161	0.173

intensity. The detector was positioned at an angle of 3°. The wavelength of the neutrons was 1.0 nm. For determining $\langle S^2\rangle_z$, a sample–detector distance of 2.7 m was chosen. Radial averaging and data treatment were performed at the ILL as usual.[36] The solvents cyclohexane-*d* and toluene-*d* were used without further purification (98% D; from Merck Sharp and Dohme, Canada).

In the low molecular weight region, the M_w data from SANS were found to lie 5–20% below those obtained from SLS experiments, which is probably due to a molecular weight dependence of the so-called contrast factor, needed for evaluating the SANS data, which, however, cannot be determined directly. We therefore only used M_w data from SLS in this paper, where the molecular weight dependence of dn/dc was taken into account. A_2 values from SANS Zimm plots are in good agreement with A_2 data from the corresponding SLS Zimm plots when A_2 from SANS was corrected by the factor $M_w(\text{SANS})/M_w(\text{SLS})$.

Estimation of Experimental Error. SLS. Molecular weights were determined with an accuracy of ±10% for the lowest and ±5% for the higher molecular weights. The error in A_2 is relatively high and may be estimated to ±10–15%. Due to the fact of a somewhat higher error in the low molecular weight region (M_w < 15000), the evaluation of A_2 is based on 9–15 different concentrations.

DLS. The diffusion coefficient can be measured with high accuracy. For the lowest M_w the error is ±6% in toluene and ±3% in cyclohexane and with increasing molecular weight the inaccuracy decreased well below ±2%. If $M_w > 20000$, a set of four different concentrations provided a determination of D sufficiently accurate, whereas in the low molecular weight region at least five different concentrations were used.

SANS. Determination of $\langle S\rangle_z^2$ is very accurate and the error is less than ±6%.

Results

Evaluation of SLS data is well-known and will not be discussed here. In DLS a time correlation function (TCF) of the scattering intensity is measured. The intensity TCF allows estimation of diffusion coefficients D_z and is determined through

$$\frac{\langle|E(0)|^2|E(t)|^2\rangle}{\langle|E(t)|^2\rangle^2} = \frac{g_2(t)}{g_2(t=\infty)} \tag{3}$$

Here, $|E(0)|^2$ and $|E(t)|^2$ are the squares of the electromagnetic field of the scattered light at time zero and t and are therefore proportional to the respective intensities. $q = (4\pi/\lambda)\sin(\theta/2)$ is the magnitude of the scattering vector. The intensity TCF, $g_2(q,t)$, is normalized to the base line, $g_2(t=\infty)$.

For small monodisperse molecules $g_2(q,t)$ can be described by a single exponential

$$g_2(q,t) = 1 + Be^{-2\Gamma t} = 1 + g_1^2 \tag{4}$$

with

$$\Gamma = Dq^2 = -\mathrm{d}\ln g_1/\mathrm{d}t \tag{5}$$

where D is the translational diffusion coefficient.

Polydispersity and intramolecular motion cause deviations from the single exponential, which can be approximated by a series expansion of $\ln g_1(q,t)$ in powers of the delay time t (cumulant expansion)

$$\ln g_1(q,t) = -\Gamma_1 t + \Gamma_2 t^2/2! \ldots \tag{6}$$

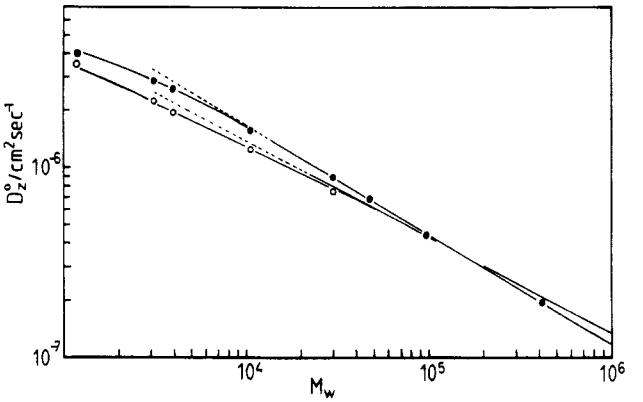

Figure 1. Plot of D_z vs. M_w: (●) PS in toluene at 20 °C; (○) PS in cyclohexane at 34.5 °C.

Table II
Results from DLS Measurements

		toluene		cyclohexane	
sample	M_w	$D_z \times 10^{-7}$, cm^2 s^{-1}	k_D, cm^3 g^{-1}	$D_z \times 10^{-7}$, cm^2 s^{-1}	k_D, cm^3 g^{-1}
WA-411	424000	1.96	70.9		
Al-1	97000	4.39	21.0		
PCC-50	48500	6.78	10.0		
Al-2	30200	8.82	5.0	7.31	−10.8
TSK-11	10700	15.7	1.7	12.30	−5.7
PCC-4	4000	25.8		19.45	−3.9
PS-3	3100	28.5		22.3	−2.8
PS-1	1200	40.1	−0.8	35.0	−2.0

where $g_1(t) = [g_2(t) - 1]^{1/2}$ and Γ_1, Γ_2, etc. are the first, second, etc. cumulants of the TCF. The PS samples used in this study are of low polydispersity ($M_w/M_n \leq 1.1$). In this case the use of eq 4 and 5 is justified, at least when we confine ourselves to the initial part of the TCF.

The first cumulant Γ_1 of the series expansion for flexible, monodisperse molecules is a function of the scattering vector q and is given by

$$\Gamma_1 = q^2 D_{app}(1 + C\langle S^2\rangle_z q^2 + \ldots) \tag{7}$$

We have investigated samples with M_w smaller than 5×10^5, and these polymers have radii of gyration too small as to produce a q^2 dependence of $\Gamma_1/q^2 \equiv D_{app}$. We therefore took the average of $D_{app} = D(c)$ measured at least for five different angles. These values of $D(c)$ are then extrapolated to the concentration $c = 0$ to give D_z at infinite dilution. See eq 2.

Figure 1 shows D_z as a function of M_w. For molecular weights larger than 30000, the molecular weight dependence of D_z in toluene can be described by

$$D_z = 3.40 \times 10^{-4} M_w^{-0.578} \tag{8}$$

For establishing this relationship we used the values of the four highest molecular weights in Table II together with the data of Bantle, Schmidt, and Burchard.[3] Equation 8 is in full agreement with literature data.[20,24] The corresponding relationship in cyclohexane is according to the literature[4-6]

$$D_z = 1.495 \times 10^{-4} M_w^{-0.508} \tag{9}$$

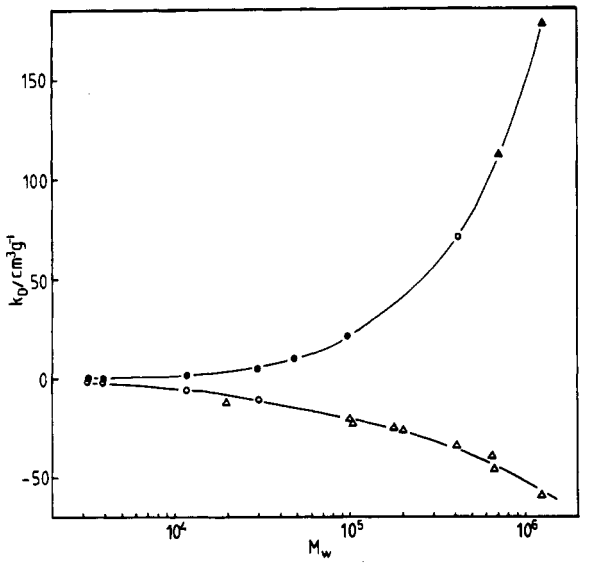

Figure 2. Experimental k_D values of PS in toluene (●) and cyclohexane (○). The plot contains in addition literature data for PS in toluene[3] (▲) and in cyclohexane[4-6] (△).

For low molecular weights, i.e., $M_w < 30000$, small but significant deviations from the simple scaling behavior

$$D_z = KM_w^{-\nu_h} \tag{10}$$

are observed in both solvents.

On the basis of the Stokes–Einstein relationship, an effective hydrodynamic radius can be defined from the translational diffusion coefficient.

$$R_h \equiv \langle 1/R_h \rangle^{-1} = kT/(6\pi\eta_0 D) \tag{11}$$

According to this relationship, the measured diffusion coefficients can be transformed into the equivalent hydrodynamic sphere radii R_h. The numerical values for $kT/(6\pi\eta_0)$ are

$$kT/(6\pi\eta_0) = 3.633 \times 10^{-13} \text{ cm} \quad \text{(toluene, 20 °C)} \tag{12}$$

$$kT/(6\pi\eta_0) = 2.997 \times 10^{-13} \text{ cm} \quad \text{(cyclohexane, 34.5 °C)} \tag{13}$$

The hydrodynamic radii will be discussed in greater detail in a separate paper, together with the concentration dependence and the effect of excluded volume on the hydrodynamic radius.

The concentration dependence of the diffusion coefficient D_{app} can be expressed by eq 2. The k_D values depend on M_w and are plotted in Figure 2 as a function of log M_w in both solvents. In addition to our own measurements the figure contains literature data.[3-6] While the cyclohexane-k_D values are all negative and increase with decreasing M_w, the corresponding data in toluene are mostly positive and reach zero values only for the lowest molecular weights ($M_w \leq 4000$).

The concentration dependence in SLS is expressed in terms of the second virial coefficient A_2, which in Figure 3 is plotted as a function of M_w. Again this plot contains data from the literature,[2,3,7,8] which are in good agreement with our own values.

As with PS in benzene,[14] the A_2 values in toluene exhibit in the low molecular weight region significant deviations upward from a straight line. In toluene the linear behavior starts already at $M_w > 10^5$ whereas in benzene this asymptote is reached when $M_w > 10^7$. For M_w larger than 10^5, A_2 in toluene can be represented by

$$A_2 = 4.362 \times 10^{-3} M_w^{-0.203} \text{ mol cm}^3/\text{g}^2 \tag{14}$$

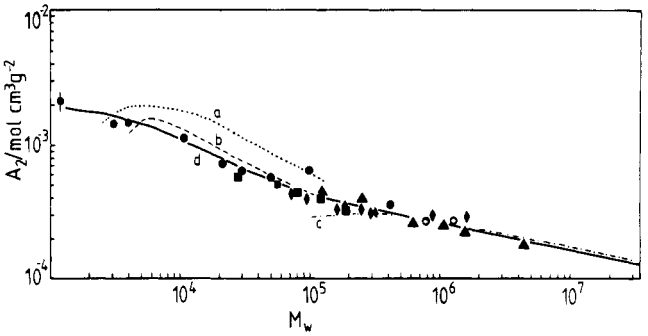

Figure 3. A_2 as a function of M_w for PS in toluene at 20 °C: (●) our measurements; (♦) Bawn et al.[7]; (■) Cowie et al.[2]; (▲) Berry et al.[8]; (○) Bantle et al.[3] Curves: (a) YS theory with $\alpha_S = \alpha_{exptl}$; (b) YS theory with $\alpha_S = \alpha_{excl}$; (c) Padé approximation 5(1,1) according to Tanaka;[15] (d) experimental curve. The bar indicates the experimental error.

Table III
Results from SLS and SANS Measurements

sample	M_w	toluene $\langle S^2\rangle_z^{1/2}$, nm	toluene $A_2 \times 10^{-4}$, cm³ mol/g²	cyclohexane $\langle S^2\rangle_z^{1/2}$, nm
WA-411	424000	28	3.5	
Al-2	97000	12	6.0	
PCC-50	48500		5.8	
Al-1	30200		6.2	
H-2	21600[a]	5.16[a]	7.3[a]	
H-1	14600[a]			3.28[a]
TSK-11	10700	3.33[a]	11.1	2.76[a]
				2.71[b]
PCC-4	4000	1.70[a]	15.0	1.53[a]
PS-3	3100	1.39[a]	14.6	1.28[a]
PS-1	1200	0.660[a]	21.7	0.654[a]

[a] Data obtained from SANS experiments. [b] SANS measurements at 38 °C.

The $\langle S^2\rangle_z$ data obtained from light scattering in the high molecular weight region exhibit the expected exponential behavior $\langle S^2\rangle^{1/2} \sim M^{\nu_S}$. In toluene[20]

$$\langle S^2\rangle_z^{1/2} = 0.0125 M_w^{0.595} \tag{15}$$

and in cyclohexane[18]

$$\langle S^2\rangle_z^{1/2} = 0.029 M_w^{0.5} \tag{16}$$

was found.

SANS measurements were carried out in the molecular weight region between 1000 and 30000 in toluene-*d* at T = 20 °C and cyclohexane-*d* at T = 35 °C. With sample TSK-11 we performed measurements at two different temperatures (35° and 38 °C) to account for the increase of the Θ point in cyclohexane-*d*.[21] No influence of the temperature on the dimensions was observed. The results are shown in Table III. They are in satisfactory agreement with the measurements of Ballard et al.[22] at T = 38 °C in cyclohexane-*d*.

Figure 4 contains plots of $\langle S^2\rangle_z^{1/2}$ vs. M_w for both solvents. The toluene data suggest an exponent ν_S significantly lower than 0.595 for a small M_w region below 10^5. In the very low molecular weight area, however, both curves exhibit a marked increase of ν_S again and seem to merge into each other at $M_w \simeq 1000$. This last observation is not in agreement with the results reported by Kirste and Wild.[23]

Discussion

Hydrodynamic Effects. The observed molecular weight dependence of D_z can as usual be described by exponential laws as long as $M_w > 30000$, where the expo-

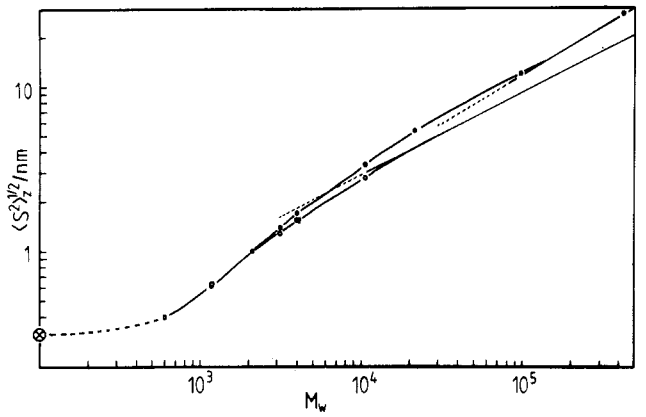

Figure 4. Plot of $\langle S^2\rangle_z^{1/2}$ vs. M_w for toluene (●) and cyclohexane (○) together with the data of Ballard et al.[22] in cyclohexane (□). (⊗) denotes an estimation of $\langle S^2\rangle^{1/2}$ of ethylbenzene as the "smallest PS".[34]

nents are $\nu_h = 0.508$ and 0.578 for cyclohexane and toluene, respectively. Note that ν_h is slightly lower than ν_S in eq 15 for toluene. The deviations to smaller values at low M_w are certainly significant and require an interpretation. Two effects have to be taken into consideration, one of hydrodynamic origin and the other caused by the directional correlation of the bonds, or, in other words, by persistence length or chain stiffness. Both effects are considered below.

To discuss the hydrodynamic effects of the chain under Θ conditions, we refer to Kirkwood's[28] theory for the translational diffusion coefficient

$$\frac{D}{kT} = \frac{1}{\zeta N} + \frac{1}{6\pi\eta_0 N^2}\sum_{i\neq j}^{N}\sum\left\langle\frac{1}{r_{ij}}\right\rangle \tag{17}$$

which also may be written as

$$\frac{D}{kT} = \frac{1}{\zeta N} + \frac{1}{3\pi\eta_0 N^2}\sum_{n=1}^{N-1}\left\langle\frac{1}{r_n}\right\rangle(N-n) \tag{18}$$

where N is the number of Kuhn segments of length l_K, which is twice the persistence length, and these Kuhn segments are assumed to be freely jointed. Under the Θ condition the segments follow a Gaussian distribution and $\langle 1/r_n\rangle$ is then given by

$$\langle 1/r_n\rangle = (6/n\pi)^{1/2} l_K^{-1} \tag{19}$$

The first term in eq 17 represents the frictional behavior of the N individual Kuhn segments, each with a friction coefficient ζ. The second term arises from the hydrodynamic interaction (HI), and the double sum is a result of Kirkwood's assumption that the total HI can be approximated by the sum over all pairs of interacting segments. Recent measurements by DLS have given evidence that the Kirkwood approximation gives too low an estimate of the total HI.[18] In the real chain this interaction appears to be larger by a factor of $\rho_{KR}/\rho_{exptl} = 1.504/1.27 = 1.18 \pm 0.03$, where $\rho \equiv \langle S^2\rangle_z^{1/2}/R_h$ and the subscript KR refers to the Kirkwood diffusion equation. In other words, the sum in eq 18 has to be divided by this factor to obtain agreement with experiment. Thus an amended equation for D takes, with eq 19 and the mentioned correction factor, the form

$$\frac{D}{kT} = \frac{1}{\zeta N} + \frac{0.124}{\eta_0 N^2 l_K}\sum_{n=1}^{N-1}(N-n)n^{-1/2} \tag{20}$$

For large N the first, free draining term can be neglected

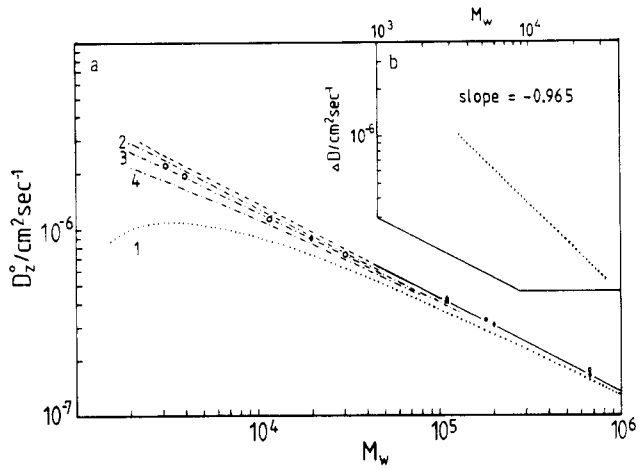

Figure 5. (a) Model calculations for D_z under Θ conditions in comparison with experimental data ((○) our values; (♦) King et al.[4]; (□) Han et al.[5] Curves: (1) nondraining term D_{ND} of the Kirkwood–Riseman theory; (2) YF theory with $d = 0.66$ nm; (3) YF theory with $d = 0.88$ nm; (4) YF theory with $d = 1.32$ nm. (b) Plot of difference $\Delta D = D_{exptl} - D_{ND}$, where D_{exptl} is given by Figure 1.

and the sum can be replaced by an integral, yielding the familiar asymptotic result

$$\lim_{N\to\infty}\frac{D}{kT} = \frac{1.27}{\langle S^2\rangle^{1/2}} \tag{21}$$

where

$$\langle S^2\rangle_0^{1/2} = (N/6)^{1/2} l_K \tag{22}$$

For short chains the sum of the nondraining part has to be evaluated exactly, which yields the dotted curve in Figure 5a. A value of $l_K = 2$ nm was used.[9] The difference between this and the measured curve, which is plotted in Figure 5b, can be interpreted as being caused by the free draining term, which should decrease as N^{-1}. To test this, we multiplied the difference curve by N, which gives an average frictional coefficient for one Kuhn segment of

$$\zeta = 93.2 \times 10^{-10}\ \text{g/s} \tag{23}$$

Applying the Stokes relationship for stick boundary condition $\zeta = 6\pi\eta_0 a$, we find for the hydrodynamic radius of a Kuhn segment $a = 0.66$ nm. Hence the hydrodynamic diameter $2a$ is of the same order as the Kuhn length of $l_K = 2$ nm reported by Fujita and Norisuye.[9] A similar procedure has been applied by Stepto and co-workers[32,33] to various systems of oligomers. Not in all examples was a full agreement with Kirkwood's relationship found, and a shift from slip to stick boundary conditions with increasing molecular weight had to be assumed by these authors.

In this estimate we have neglected the non-Gaussian behavior of the short chains. Still the hydrodynamic properties can surprisingly well be described by a Gaussian chain, if the Kuhn segment is chosen as the basic element in a pearl necklace model and chain stiffness is absorbed completely by this subunit. According to the analysis of the radii of gyration by Fujita and Norisuye,[9] chain stiffness becomes noticeable below $M_w = 30\,000$, i.e., $N < 35$.

For the second approach we chose the theory of the translational friction coefficient of wormlike chains by Yamakawa and Fujii.[10] This theory is based on the Oseen–Burgers[11,12] procedure for calculating the frictional force of a continuous cylinder with the reduced contour length $L = L_{cont}/l_K$ and the reduced chain diameter $d = d_{cyl}/l_K$, where L_{cont} and d_{cyl} are actual contour length and

chain diameter. For the derivation of the mean reciprocal distance between points on the cylinder surface and the cylinder axis, the authors apply the second Daniels approximation[29] for the distance distribution if $L > 2.278 \equiv \sigma$. For shorter distances they use the empirical cubic approximation of Hearst and Stockmayer.[13] After integration over all cylinder distances they arrive at the following two equations:

For $L > \sigma$:

$$(D/kT)(3\pi\eta_0 L) = A_1 L^{1/2} + A_2 + A_3 L^{-1/2} + A_4 L^{-1} + A_5 L^{-3/2} \quad (24)$$

and

For $L < \sigma$:

$$(D/kT)(3\pi\eta_0 L) = C_1 \ln (L/d) + C_2 + C_3 L + C_4 L^2 + C_5 L^3 + C_6 (d/L) \ln (L/d) + C_7 (d/L) + C_8 (d/L)^2 + C_9 (d/L)^3 + C_{10} (d/L)^4 \quad (25)$$

where all the coefficients A_j and C_j except A_1 are functions of the reduced cylinder diameter d. Equation 24 approaches for long chains the Kirkwood asymptote of Gaussian coils, which is larger by the factor 1.18 than that found experimentally. To correct for this fact, we changed the coefficient A_1, which is the only factor remaining effective in the Gaussian limit, and we used $A_1 = 1.561$ instead 1.843 as given by the authors[10] in their eq 50.[38] Likewise it may be justified to correct all the coefficients A_j and C_j by the same factor. This procedure, however, which necessarily is required for $L < \sigma$, gives a noticeable change only if the chain diameter d is larger than 1 nm, i.e., for curve 4 in Figure 5, but does not change the interpretation.

The Yamakawa–Fujii (YF) equations contain the Kuhn length l_K, the reduced contour length L (i.e., the number of Kuhn lengths per chain), and the reduced diameter, which is $d = 2r/l_K$, with $2r$ the actual diameter. A Kuhn length of $l_K = 2$ nm was taken from Norisuye and Fujita[9] and L was calculated from the molecular weight of the wormlike chain by the relationship

$$L = M_w l_K^{-1}/M_L \quad (26)$$

where $M_L = 390$ g/(mol nm) is the mass per unit length and was again taken from Norisuye and Fujita. Hence only d or $2r$ enters the YF theory as an adjustable parameter. Since it appeared to us conceivable that a bead of the hydrodynamic volume $4\pi a^3/3 = V_h$(Kirkwood–Riseman)[28] could be equivalent to the hydrodynamic volume of the cylindrical Kuhn segment $(d/2)^2\pi l_K = V_h$(Yamakawa–Fujii),[10] we used this equivalence to estimate reasonable values for the adjustable parameter r.

$$r = [(4/3)a^3/l_K]^{1/2} \quad (27)$$

From eq 27 with $a = 0.66$ nm and $l_K = 2$ nm a value of 0.88 nm for $2r$ is obtained. We have carried out calculations with $2r = 0.66$, 0.88, and 1.32 nm, respectively, which are drawn in Figure 5a. The best fit is obtained with $2r = 0.88$ nm.

In conclusion, we observe that both approaches, that of the Kirkwood model containing a free draining term, on the one hand, and that of the YF theory of a wormlike chain, on the other, give a very good description of the diffusion coefficient, when in both cases the Gaussian limit is corrected for a higher hydrodynamic interaction by a factor of 1.18 ± 0.03. At first sight the agreement of both theories is a little unexpected, since the YF theory contains no explicit free draining term. Instead of this an effective chain diameter is used. A clear separation of the free draining and nondraining contribution to the friction coefficient is no longer feasible in the YF theory. The role of the free draining term has been discussed in some detail by Yamakawa and Fujii. In addition to that, we may remark that the free draining term can be transformed by eq 27 into the actual chain diameter ($=2r$), which turns out to be equivalent to the diameter in the YF theory.

Excluded Volume Effects. Next we discuss the molecular weight dependence of the second virial coefficient, for which exact knowledge of the behavior of $\langle S^2\rangle_z^{1/2}$ in the low molecular weight region is essential. The exponent -0.2 in the asymptotic behavior at large M_w is easily understood from current theories of A_2, which can be written as

$$A_2 = 4\pi^{3/2} N_A \langle S^2\rangle^{3/2} \psi(\bar{z})/M^2 \quad (28)$$

where[17]

$$\bar{z} = z/\alpha_S^3 \quad (29)$$

and

$$z = n^{1/2}\beta(3/2\pi b^2)^{3/2} \quad (30)$$

At large values of z, i.e., at high molecular weight, the interpenetration function $\psi(\bar{z})$ becomes independent of $\bar{z}$ or molecular weight. In a good solvent we have

$$\langle S^2\rangle^{3/2} \sim M^{1.8} \quad (31)$$

and therefore with eq 28 asymptotically

$$A_2 \sim M^{-0.2}\psi(\bar{z}) \quad (32)$$

For short chains the function $\psi(\bar{z})$ decreases to zero. This implies deviations of the A_2 vs. M_w curve from the straight line toward *smaller* values. Numerical calculations on the basis of the Padé approximation by Tanaka,[15] indicated by curve c of Figure 3, show indeed a decrease of A_2 for $M_w < 10^5$. For details of the calculation see Appendix 1. Hence the observed upturn must result from other sources.

At intermediate chain length the interpenetration factor $\psi(\bar{z})$ passes through a flat maximum which appears significantly out of the experimental error limit. The maximum in $\psi(\bar{z})$ is in turn correlated to the early deviations of A_2 from the asymptote of eq 32 toward higher values. The parameter $\bar{z}$ can change its value by variation of the molecular weight, i.e., $n^{1/2}$, in a fixed solvent or by alteration the solvent quality, i.e., β, for a given molecular weight. There is some evidence that the flat maximum occurs only on altering $\bar{z}$ via $n^{1/2}$ but not via variation of β. A similar maximum for $\psi(\bar{z})$ was observed many years ago for poly(vinylpyrrolidone) solution.[30]

It is worth mentioning that the experimental A_2 data of PS in benzene as a function of M_w exhibit a similar upturn at small molecular weights.[14] This upturn causes again a distinct maximum of $\psi(\bar{z})$ at intermediate values of $\bar{z}$. One may conclude from this observation that the current theories on the interpenetration factor are incorrect for short chains, because all these considerations are based on the assumption of ideally flexible random coils, which, however, must fail for short chains in view of the inherent chain stiffness. We thus tried to calculate A_2 for very short chains on the basis of the Yamakawa–Stockmayer[16] perturbation theory for wormlike chains.

The molecular weight dependences of $\langle S^2\rangle_z^{1/2}$ for PS in toluene and cyclohexane have been used to determine "experimental" α_S values. These α_S values, called α_{exptl}, were then taken for the calculation of A_2 according to the YS theory in the molecular weight region between 10^3 and 10^5 (details in Appendix 2).

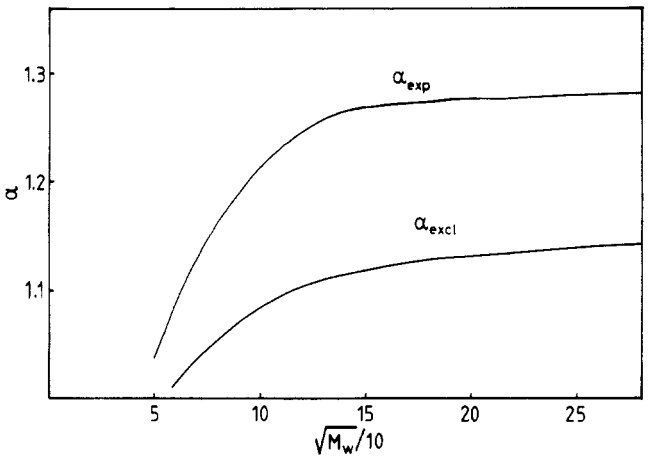

Figure 6. Interpolated behavior of α_{exptl} obtained from Figure 4 and α_{excl} defined by eq 33 and 36.

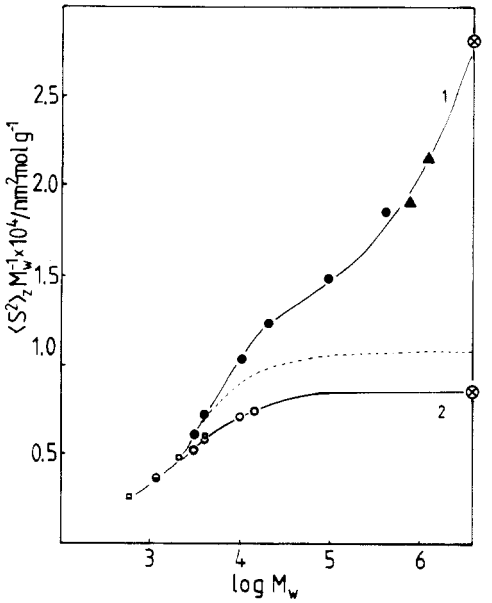

Figure 7. $\langle S^2\rangle_z/M_w$ vs. log M_w in toluene (1) and cyclohexane (2); (⊗) were calculated from eq 15 and 16, respectively. The dashed curve was calculated by eq 33 and 36.

As seen in Figure 3, these A_2 values lie significantly above the experimental data. This behavior indicates that α_{exptl} is larger than expected from excluded volume effects only. Evidently α_{exptl} contains a factor α_{ud} which arises from differences in the unperturbed dimensions and α_{exptl} may be written as

$$\alpha_{exptl} = \langle S^2\rangle_z^{1/2}/\langle S^2\rangle_{z\theta}^{1/2} \equiv \alpha_{ud}\alpha_{excl} \quad (33)$$

Plots of α_{exptl} as a function of $M_w^{1/2}$ and $\langle S^2\rangle_z/M_w$ as a function of log M_w are shown in Figures 6 and 7. The curves exhibit plateau regions in the molecular weight range between 20 000 and 100 000, which is characteristic for unperturbed Gaussian chains. However, the corresponding plateau for PS in cyclohexane is about 2 times lower.

In a first approach we considered the higher plateau as being caused by a higher persistence length alone and calculated for the region $M < 10^5$ new values for the mass per length M_L and the Kuhn length l_K using the relationship of Norisuye et al.[9] for the characteristic ratio C_∞ and $M_{1/2}$

$$C_\infty = l_K/(6M_L) \quad (34)$$

$$M_{1/2} = 7.08 l_K M_L \quad (35)$$

where $M_{1/2}$ denotes the value of M_w at which $\langle S^2\rangle_z/M_w$ equals $C_\infty/2$. The so calculated Kuhn length in toluene is 2–2.5 times larger than found in cyclohexane. Correspondingly, M_L increases from 390 in cyclohexane to 500–590 g/(mol nm) in toluene. No satisfactory description of the experimental data in this region was possible with the Yamakawa–Stockmayer theory under the assumption that $\alpha_{excl} \simeq 1$ and $\bar{z} \simeq z$.

In the second approach, we assumed α_{exptl} being influenced by both a change in chain stiffness and excluded volume. Then choosing values l_K and M_L in between the two extremes ($\alpha_{exptl} = \alpha_{ud}$ and $\alpha_{exptl} = \alpha_{excl}$), i.e., $l_K = 2.90$ nm and $M_L = 450$ g/(mol nm), unperturbed radii of gyration $\langle S^2\rangle^{1/2}$ were calculated by means of the Benoit–Doty expression.[31]

$$\langle S^2\rangle/l_K^2 = (n_K/6) - (1/4) + 1/(4n_K) - (1 - e^{-2n_K})/(8n_K^2) \quad (36)$$

These calculated data together with the experimental values in toluene now allow estimation of α_{excl}. These α_{excl} values together with the altered Kuhn length were fed into the YS theory to calculate A_2 (Appendix 2). A much better fit of the experimental data is now obtained. This strongly supports the assumption of a simultaneous action of chain stiffness and excluded volume on α_{exptl}. Also the upturn of A_2 in the low molecular weight region appears now to be caused by the chain stiffness.

The solvent may influence a change in the short-range interaction and thus the unperturbed dimensions. The assumed increase of 45% nevertheless is fairly high, and we do not put too much emphasis on the accurate value. We only wish to point out that a satisfactory description of experimental A_2 data is obtained by the assumption of a change in the unperturbed dimensions, which otherwise cannot be achieved.

At the end of this discussion we wish to remark that a very good description of the molecular weight dependence is obtained with the simple relationship of A_2 for spheres

$$A_2 = 4N_A v_m/M^2 \quad (37)$$

if the volume of the sphere is taken as the hydrodynamically effective volume, i.e.

$$v_m = v_h = 4\pi R_h^3/3 \quad (38)$$

This unexpected behavior seems to indicate that the thermodynamic interaction is very close to the hydrodynamic one. This relationship will be examined in a separate paper.

Acknowledgment. We are indebted to Professor H. Höcker, University of Bayreuth, for supplying us with two low molecular weight PS samples. We also thank Dr. Manfred Schmidt, Max-Planck Institut für Polymerforschung, Mainz, and Professor A. Z. Akcasu (University of Michigan) for many valuable discussions. The work was kindly supported by the Deutsche Forschungsgemeinschaft within the scheme of the SFB 60.

Appendix 1

The main problem in calculating A_2 from Padé approximation consists in the determination of the z parameter as a function of M_w. To this end we first determined from experimental data of $\langle S^2\rangle_z$ in toluene[3,19,20] and cyclohexane[18] at 34 °C the expansion factors α_S. Then we entered the Padé approximations 5(2,2) and 5(1,1) for α_S given by Tanaka[15]

$$\frac{\alpha_S^5 - 1}{z} = \frac{67(1 + 2.501z)}{21(1 + 3.177z)} \quad (A.1)$$

$$(\alpha_S^5 - 1)/z = 67/21 \quad \text{(A.2)}$$

from which the desired M_w dependence of z could be obtained and which seems to be the best approach in the high molecular weight region.

These z values were then inserted into eq 7 of Tanaka[15]

$$h(z) = (1 + 7.16z)^{-2/5} \quad \text{(A.3)}$$

and with this function we eventually calculated $\psi(z)$ and A_2 as a function of M_w.

Appendix 2

To calculate A_2 for short stiff chains, we used a procedure worked out by Yamakawa and Stockmayer.[16] With their eq 119, the function $H(L,d)$ was calculated, where L is the contour length and d the thickness of the chain (=0.88 nm).

With the aid of α_S data, interpolated from experimental data, we can estimate reasonable values for z by use of

$$\alpha_S^5 - \alpha_S^3 = (67/70)Kz \quad \text{(A.4)}$$

where K is given by their eq 83 with eq 85.

Now we were able to calculate the interpenetration function $\psi(\bar{z})$, where $\bar{z}$ is defined as

$$\bar{z} = z/\alpha_S^3 \quad \text{(A.5)}$$

$$Q(L) = 2L^{-5/2}H(L,d) \quad \text{(A.6)}$$

$$\bar{z}h(\bar{z}) = (2Q)^{-1} \ln (1 + 2Qz) \quad \text{(A.7)}$$

$$\psi(\bar{z}) = (\langle S^2\rangle_0/\langle S^2\rangle_{z\theta})^{3/2}\bar{z}h(\bar{z}) \quad \text{(A.8)}$$

$\langle S^2\rangle_{z\theta}/\langle S^2\rangle_0$ is the ratio of the mean square radius of gyration to the Gaussian coil limit value $\langle S^2\rangle_0$ according to eq 22. A_2 is calculated by

$$A_2 = (4\pi^{3/2}N_A\langle S^2\rangle^{3/2}/M^2)\psi(\bar{z}) \quad \text{(A.9)}$$

Registry No. PS (homopolymer), 9003-53-6; neutron, 12586-31-1.

References and Notes

(1) ter Meer, H.-U.; Burchard, W.; Wunderlich, W. *Colloid Polym. Sci.* **1980**, *285*, 675.
(2) Cowie, J. M. G.; Worsfold, D. J. *Trans. Faraday Soc.* **1961**, *57*, 705.
(3) Bantle, S.; Schmidt, M.; Burchard, W. *Macromolecules* **1982**, *15*, 1604.
(4) King, T. A.; Knox, A.; Lee, W. I.; McAdam, J. D. C. *Polymer* **1973**, *14*, 151.
(5) Han, C. C.; McCrackin, F. L. *Polymer* **1979**, *20*, 427.
(6) Jones, G.; Caroline, J. *J. Chem. Phys.* **1979**, *37*, 187.
(7) Bawn, C. E. H.; Wajid, M. A. *J. Polym. Sci.* **1957**, *12*, 109.
(8) Berry, G. C. *J. Chem. Phys.* **1966**, *44*, 4550.
(9) Norisuye, T.; Fujita, H. *Polym. J.* **1982**, *14*, 143.
(10) Yamakawa, H.; Fujii, M. *Macromolecules* **1973**, *6*, 407.
(11) Oseen, C. W. "Hydrodynamik"; Akademische Verlagsgesellschaft: Leipzig, 1927.
(12) Burgers, J. M. "Second Report on Viscosity and Plasticity of the Amsterdam Academy of Sciences"; Nordemann: New York, 1983, Chapter 3.
(13) Hearst, J. E.; Stockmayer, W. H. *J. Chem. Phys.* **1962**, *37*, 1425.
(14) Miyaki, Y.; Einaga, Y.; Fujita, H. *Macromolecules* **1978**, *11*, 1180.
(15) Tanaka, G. *J. Polym. Sci., Polym. Phys. Ed.* **1979**, *17*, 305.
(16) Yamakawa, H.; Stockmayer, W. H. *J. Chem. Phys.* **1972**, *57*, 2843.
(17) Yamakawa, H. "Modern Theory of Polymer Solutions"; Harper and Row: New York, 1971.
(18) Schmidt, M.; Burchard, W. *Macromolecules* **1981**, *14*, 210.
(19) Huber, K. Diploma Thesis, Freiburg, 1982.
(20) Raczek, J. Dissertation, Mainz, 1980.
(21) Strazielle, C.; Benoit, H. *Macromolecules* **1975**, *8*, 203.
(22) Ballard, D. G. H.; Rayner, M. G.; Schelten, J. *Polymer* **1976**, *17*, 349.
(23) Kirste, R. G.; Wild, G. *Makromol. Chem.* **1969**, *121*, 174.
(24) Appelt, B.; Meyerhoff, G. *Macromolecules* **1980**, *13*, 657.
(25) Meyerhoff, G.; Schulz, G. V. *Makromol. Chem.* **1951**, *7*, 294.
(26) Flory, P. J. "Principles of Polymer Chemistry"; Cornell University Press: Ithaca, NY, 1953.
(27) Burchard, W.; Schmidt, M.; Stockmayer, W. H. *Macromolecules* **1980**, *13*, 580, 1265.
(28) Kirkwood, J. G.; Riseman, J. *J. Chem. Phys.* **1948**, *16*, 565.
(29) Daniels, H. E. *Proc. R. Soc. London, Ser. A* **1952**, *63*, 290.
(30) Burchard, W. Habilitationsschrift, Freiburg, 1966.
(31) Benoit, H.; Doty, P. *J. Chem. Phys.* **1953**, *57*, 958.
(32) Mokrys, I. J.; Rigby, D.; Stepto, R. F. T. *Ber. Bunsenges. Phys. Chem.* **1979**, *83*, 446.
(33) Edwards, C. J. C.; Rigby, D.; Stepto, R. F. T. *Macromolecules* **1981**, *14*, 1808.
(34) Bantle, S., unpublished data.
(35) Institut Max von Laue-Paul Langevin, "Neutron Beam Facilities Available for Users", Jan 1981 edition.
(36) Ghosh, R. E. "A Computing Guide for SANS Experiments at the ILL", 1981, GH 29T.
(37) Dandliker, W. B.; Krautt, J. *J. Am. Chem. Soc.* **1956**, *78*, 2380.

(38) A change of the value for A_1 requires a corresponding change of the coefficients C_i in eq 25, which guarantees that the two curve sections of eq 24 and 25 have at $L = \sigma$ the same value and the same derivative. Since, however, in the present treatment eq 25 was not needed, we did not carry out the corresponding alteration.

Detailed Molecular Structure of a Vinyl Polymer Glass

Doros N. Theodorou and Ulrich W. Suter*

Department of Chemical Engineering, Massachusetts Institute of Technology, Cambridge, Massachusetts 02139.

Received November 9, 1984

ABSTRACT: A method is developed for the detailed atomistic modeling of well-relaxed amorphous glassy polymers. Atactic polypropylene at −40 °C is used as an example. The model system is a cube with periodic boundaries, filled with segments from a single "parent" chain. An initial structure is generated by using a modified Markov process, based on rotational isomeric state theory and incorporating long-range interactions. This structure is then "relaxed" by potential energy minimization, using analytical derivatives. Computing time is kept relatively small by stagewise minimization, employing a technique of "blowing up" the atomic radii. Model estimates of the cohesive energy density and the Hildebrand solubility parameter agree very well with experiment. The conformation of the single chains in the relaxed model system closely resembles that of unperturbed chains. Pair distribution functions and bond direction correlation functions show that the predominant structural features are intramolecular and that long-range orientational order is completely absent.

Introduction

An accurate description of glassy polymers in detailed molecular terms is not available to date, and as a result there is no theoretical treatment of deformation and relaxation phenomena in polymeric glasses based on "first principles"; consequently, phenomenological concepts[1]

0024-9297/85/2218-1467$01.50/0